Experimental Investigation of Surface Preparation on Normal and Ultrahigh-Performance Concrete Interface Behavior

Sumedh Sharma[1]; Vidya Sagar Ronanki[2]; Sriram Aaleti, M.ASCE[3]; and Pinar Okumus, A.M.ASCE[4]

Abstract: Many bridges in the United States are classified as structurally deficient and many others are nearing the end of their design service life, necessitating robust and durable bridge rehabilitation methodologies. States' department of transport have recently developed innovative solutions for accelerated bridge construction using Ultrahigh Performance Concrete (UHPC) as grout material between prefabricated bridge components or as an overlay over existing bridge decks to increase their service life. The normal strength concrete (NSC)-UHPC interface behavior is critical in determining the overall performance of such NSC-UHPC composites. In this study, an experimental investigation was performed to quantify the effect of surface preparation and interface reinforcement on NSC-UHPC interface performance. The results from this study were compared with the current design guidelines for estimating interface shear capacity. In general, it can be concluded that increasing roughness depth and reinforcement area has a positive effect in interface shear capacity.
DOI: 10.1061/(ASCE)BE.1943-5592.0001697.

Author keywords: Ultrahigh performance concrete (UHPC); Interface bond; Accelerated bridge construction; Shear friction; Bridge repair.

Introduction

As of 2016, nearly 9.1% of the bridges in the United States were classified as structurally deficient, with the average age of the bridges reaching 43 years. Almost 39% of bridges were past the design service life of 50 years, and 10% of total bridges had weight or speed restrictions. The structurally deficient bridges themselves had, on average, 188 million trips each day (ASCE 2017). These bridge infrastructure challenges show a need for robust and durable rehabilitation methods for structurally deficient bridges and innovative accelerated bridge construction (ABC) practices for shorter construction times. These advancements are also necessary to increase emphasis on work zone safety, reduce users cost associated with traffic delays, and decrease the environmental impacts of the construction process (Aaleti and Sritharan 2014).

In recent years, the Federal Highway Administration (FHWA) has been seeking a balanced approach to preservation and replacement of structurally deficient and obsolete bridges. The goal has been to employ cost-effective strategies and actions to maximize the useful life of bridges while also seeking a means of decreasing construction time for new structures (FHWA 2011). For the preservation of existing bridges, bonded concrete overlays are frequently used to repair and strengthen structurally deficient concrete bridge decks and concrete pavements. The effectiveness and durability of the method is dependent on superior material properties of the repair layer and a good interface bond between the base layer and the concrete overlay. Material properties and interface bond are important for obtaining monolithic action between the two concrete layers, promoting crack control in the overlay, and preventing transport of water and detrimental substances in the interface between the two layers (Silfwerbrand 2017). For replacement of existing bridges, the use of prefabricated, full-depth precast concrete deck systems can accelerate the construction or replacement of bridge decks significantly while extending the service life and minimizing the life-cycle costs of the bridge decks (Berger 1983). Durable and efficient connections between precast bridge deck panels are needed to overcome serviceability challenges caused by cracking and poor construction of connections.

Ultrahigh performance concrete (UHPC), which is a new class of concrete that exhibits superior mechanical and durability properties, is being used as an overlay to repair deficient normal strength concrete (NSC) bridge decks and as a field-cast closure pour or grout material in bridge connections. The interface bond capacity between precast concrete and field-cast UHPC is critical in determining the overall strength and durability of such composites. The interface bond strength should resist the stresses developed due to mechanical and thermal loads while also maintaining an extended service-life performance (Munoz et al. 2014). The shear stress transfer mechanism between two concrete layers is complex and is governed by different factors such as the amount of reinforcement crossing the interface, the compression resistance of the weaker concrete, the roughness of the interface, and the compressive stress generated by normal forces across the interface. Hence, it is important to understand NSC-UHPC interface shear behavior under varying loading conditions, varying surface roughness and preparation, and varying strength and thickness of concrete layers. For the remainder of the paper, whenever a composite is described by acronyms such as "NSC-UHPC," the first term denotes concrete that was cast first.

Interface Shear Friction

Shear-friction theory was developed in the 1960s by Birkeland and Birkeland (1966), Mast (1968), and Hofbeck et al. (1969)

[1]Graduate Student, Dept. of Civil, Construction and Environmental Engineering, Univ. of Alabama, 2024 SERC Building, Tuscaloosa, AL 35401. Email: ssharma11@crimson.ua.edu

[2]Bridge Engineer, TY Lin International, 12011 Bel-Red Rd #203, Bellevue, WA 98005. Email: visa.ronanki@tylin.com

[3]Associate Professor, Dept. of Civil, Construction, and Environmental Engineering, Univ. of Alabama, 2037 C SERC Building, Tuscaloosa, AL 35401 (corresponding author). ORCID: https://orcid.org/0000-0002-8738-454X. Email: saaleti@eng.ua.edu

[4]Associate Professor, Dept. of Civil, Structural and Environmental Engineering, Univ. at Buffalo, 222 Ketter Hall, Buffalo, NY 14260. Email: pinaroku@buffalo.edu

Note. This manuscript was submitted on November 2, 2019; approved on October 28, 2020; published online on January 20, 2021. Discussion period open until June 20, 2021; separate discussions must be submitted for individual papers. This paper is part of the ***Journal of Bridge Engineering***, © ASCE, ISSN 1084-0702.

to estimate the interface shear capacity between precast elements and a nonmonolithically poured layer of concrete. Shear-friction theory estimates the interface shear resistance in terms of friction force across a roughened surface. This concept is explained by a sawtooth model presented by Birkeland and Birkeland (1966). Shear loading causes longitudinal slip across the interface after overcoming aggregate interlock, which results in displacement in the transverse direction. This displacement results in tension force in interface steel reinforcement. The tension force developed in the reinforcement causes normal clamping forces across the interface. The friction force is the product of the normal clamping forces across the interface and the tangent of the contact angle across the surface. ACI 318-14 (ACI 2014), AASHTO (2017), and PCI (2010) utilize the same basic principle to calculate the interface shear capacity.

The shear friction theory has been continuously studied since the 1960s by several researchers. The current understanding of the shear force transfer mechanism across a concrete interface has evolved to include the contributions due to adhesion, shear friction, and dowel action (Santos and Julio 2014). The adhesion component is initiated by chemical bonds established between the particles of old and new concrete. When the shear stress exceeds the adhesion capacity, debonding between the substrate and the overlay occurs at the interface. After debonding, the shear stress is transferred by mechanical interlocking generated by surface preparation. With the increase in interface slip, the reinforcement will provide normal clamping forces across the interface. Owing to relative slip along the interface, the shear reinforcement will also be subjected to shear, usually referred to as the dowel action. AASHTO code provisions consider both cohesion and friction capacity separately and their sum. ACI and PCI guidelines ignore the cohesion term and rely on the friction capacity alone. AASHTO, ACI, and PCI provisions implicitly assume yield of interface reinforcement at peak shear capacity for reinforcement up to Grade 60 [i.e., yield strength of 414 MPa (60 ksi)]. The equations from the aforementioned guidelines are listed in Table 1.

Ultrahigh Performance Concrete

UHPC is defined as a cementitious material consisting of discontinuous fibers, which has compressive strengths above 150 MPa (21.7 ksi), and pre- and postcracking tensile strengths above 5 MPa (0.72 ksi) (FHWA 2013). UHPC formulation often consists of a combination of Portland cement, fine sand, silica fume, high range water-reducing admixture (HRWR), fibers (usually steel), and water (FHWA 2013). Some of the notable differences between UHPC and NSC composition are lack of coarse aggregates, addition of steel fibers, high proportions of cementitious materials, and a low water–cement ratio. The use of powder and well-graded constituents assists to achieve a high packing density in UHPC. This leads to significantly improved mechanical properties, such as increased compressive strength and tensile strength compared with NSC (FHWA 2013). In addition, dense cement matrix creates low permeability concrete, which greatly enhances its resistance to corrosion and degradation. The use of steel fibers in UHPC helps in increasing the material's ductility as well as its tensile capacity. UHPC also displays a self-consolidating/self-leveling behavior, which allows it to be placed in plant and under field conditions with little or no vibration, leading to reduced construction costs. The improved mechanical properties of UHPC allows designers to use it in a thin layer as repair overlay, decreasing dead load on the structure and improving overall structural efficiency. UHPC also displays rapid early strength gain, which helps in expediting construction. A commercial UHPC mix (Ductal) provided by Lafarge North America was used in the experimental study presented in this paper.

Previous Research on Interface Shear Strength Involving UHPC

A summary of experimental research available in literature on quantifying interface shear strength involving NSC and UHPC is presented in this section. Banta (2005) carried out 24 push-off tests using UHPC-lightweight concrete (LWC) composites, investigating the impact of design parameters such as specimen size, reinforcement

Table 1. Design equations for interface shear strength in design guidelines

Interface condition	AASHTO LRFD (8th ed.) (5.7.4.3)	ACI 318-14 (22.9.4)	PCI 7th ed. (5-32a)
Equations	$V_{ni} = cA_{cv} + \mu(A_{vf}f_y + P_c)$	$V_{ni} = \mu A_{vf} f_y$	$V_{ni} = \mu A_{vf} f_y$
Limitations	$V_{ni} \le K_1 f'_c A_{cv}$ $V_{ni} \le K_2 A_{cv}$ $A_{vf} \ge 0.05\ A_{cv}/f_y$ and $f_y \le 414$ MPa (60 ksi)	For monolithic or roughened surface cases $V_{ni} \le (3.31 + 0.08 f'_c) A_{cv}$ For all the cases $V_{ni} \le K_1 f'_c A_{cv}$ $V_{ni} \le K_2 A_{cv}$ and $f_y \le 414$ MPa (60 ksi)	$V_{ni} \le K_1 f'_c A_{cv}$ $V_{ni} \le K_2 f'_c A_{cv}$
1. Concrete placed monolithically	$c = 2.76$ MPa (400 psi) $\mu = 1.4$; $K_1 = 0.2$ $K_2 = 10.34$ MPa (1,500 psi)	$\mu = 1.4$; $K_1 = 0.2$ $K_2 = 11.03$ MPa (1,600 psi)	$\mu = 1.4$; $K_1 = 0.3$ $K_2 = 6.9$ MPa (1,000 psi)
2. Cast in place slab on clean concrete, 6.4 mm (0.25 in.) amplitude roughness surface	$c = 1.65$ MPa (240 psi) $\mu = 1.0$; $K_1 = 0.25$ $K_2 = 10.34$ MPa (1,500 psi)	$\mu = 1.0$; $K_1 = 0.2$ $K_2 = 11.03$ MPa (1,600 psi)	$\mu = 1.4$; $K_1 = 0.25$ $K_2 = 6.9$ MPa (1,000 psi)
3. Concrete placed against hardened concrete not intentionally roughened	$c = 0.52$ MPa (75 psi) $\mu = 0.6$; $K_1 = 0.2$ $K_2 = 5.52$ MPa (800 psi)	$\mu = 0.6$; $K_1 = 0.2$ $K_2 = 5.52$ MPa (800 psi)	$\mu = 0.6$; $K_1 = 0.2$ $K_2 = 5.52$ MPa (800 psi)
4. Concrete to steel	$c = 0.17$ MPa (25 psi) $\mu = 0.7$; $K_1 = 0.2$ $K_2 = 5.52$ MPa (800 psi)	$\mu = 0.7$; $K_1 = 0.2$ $K_2 = 5.52$ MPa (800 psi)	$\mu = 0.7$; $K_1 = 0.2$ $K_2 = 5.52$ MPa (800 psi)

Note: A_{cv} = area of shear interface; A_{vf} = area of interface shear reinforcement; P_c = permanent net compressive force; f_y = yield strength of interface shear reinforcement; μ = coefficient of friction; c = cohesion factor; K_1 = fraction of concrete strength available to resist interface shear; and K_2 = limiting interface shear resistance.

ratio, and surface preparation. They found that roughening the interface increased the interface shear capacity. In specimens with a smooth interface, increasing the reinforcement ratio by six times, increased the shear capacity from 1.17 MPa (0.17 ksi) to 2.62 MPa (0.38 ksi), a 220% increase. Crane (2010) performed push-off tests on UHPC-high performance concrete (HPC) composites with varying surface preparation and reinforcement ratios. The average interface shear capacity for UHPC-HPC composites for smooth, burlap roughened and 6.35 mm (0.25 in.) fluted specimens without interface reinforcement was found to be 1.10 MPa (0.16 ksi), 2.56 MPa (0.37 ksi), and 3.72 MPa (0.54 ksi), respectively. In specimens with a smooth interface, Crane (2010) concluded that a linear increase in shear capacity from 2.21 MPa (0.32 ksi) to 4.21 MPa (0.61 ksi) was observed when the reinforcement ratio tripled. Both Banta (2005) and Crane (2010) found ACI and AASHTO design recommendations conservative in estimating shear capacity.

Sarkar (2010) performed slant shear tests on NSC-UHPC composites with different surface preparations. The specimens with no surface preparation failed along the interface while the specimens with interface roughness failed through compression of the NSC substrate. The interface strength in specimens with 2 mm (0.08 in.) deep chipped interface, 5 mm (0.20 in.) deep grooved interface, and 13 mm (0.5 in.) deep shear key at interface was found to be 28%, 56%, and 57% higher than that of specimens with a smooth interface. Munoz et al. (2014) also carried out slant shear tests on NSC-UHPC composites with a focus on quantifying the impact of interface preparation and interface angle on interface strength. Four different interface textures (brushed, sandblasted, grooved, exposed aggregate), three different NSC concrete mixes [44.54 MPa (6.45 ksi), 45.55 MPa (6.60 ksi), and 55.93 MPa (8.11 ksi)], and two different interface angles (60° and 70°) were used in slant shear tests. All specimens with an interface angle of 60° failed in the concrete substrate. For specimens with an interface angle of 70°, the brushed specimens experienced bond failures while the specimens with other surface preparations mostly failed in the concrete substrate.

Jang et al. (2017) studied the interface shear strength of UHPC-UHPC and NSC-UHPC composites using push-off tests. Five types of construction joints, namely, vertical joint, water jetted joint, and joints with three different groove sizes, were used in the study. The researchers observed that in UHPC-UHPC specimens, interface strength and ductility were enhanced by fiber distribution in the grooves across the interface. In case of NSC-UHPC specimens, aggregate interlock due to water jetting enhanced the interface strength. For specimens with 30 mm (1.2 in.) deep grooved interface, interface shear strengths in UHPC-UHPC and NSC-UHPC specimens were found to be 14.83 MPa (2.15 ksi) and 5.13 MPa (0.74 ksi), respectively. In specimens for which the joint was prepared by water jetting, the measured interface shear capacities for UHPC-UHPC and NSC-UHPC were 6.06 MPa (0.88 ksi) and 6.02 MPa (0.87 ksi), respectively.

Aaleti and Sritharan (2019) performed slant shear tests and three-point bending tests on NSC-UHPC composite specimens with varying interface roughness, pouring sequence, and NSC substrate strengths. Sixty slant shear composite specimens were cast using five different texture depths varying from 1.26 mm (0.05 in.) to 6.5 mm (0.26 in.). The NSC substrate had strength varying from 34 MPa (4.9 ksi) to 52 MPa (7.5 ksi). In general, specimens with a roughness lower than 1.59 mm (0.063 in.) experienced sliding failure at the interface while specimens with a rougher texture failed within the NSC substrate. Based on the findings, the authors conclude that a minimum roughness of 1.59 mm (0.063 in.) is sufficient to develop adequate bond strength in the NSC-UHPC composite under combined shear and compression loading. The authors did not find a significant influence of pouring sequence on bond strength. For three-point bending tests, four NSC-UHPC composites and a specimen with standard concrete overlay were tested to evaluate the interface bond strength under flexural loading. Texture depths varying from 1.26 mm (0.05 in.) to 5 mm (0.196 in.) were used in the interface. The specimens failed due to shear failure in the NSC substrate. The minimum interface bond stress at shear failure of the NSC substrate ranged from 1.31 MPa (0.19 ksi) to 1.48 MPa (0.22 ksi).

Research Need and Scope

As summarized previously, earlier studies have shown an excellent bond between UHPC and normal concrete when adequate interface roughness is provided. However, there are limited tests on NSC-UHPC specimens under direct shear and four-point bending. The previous direct shear tests conducted on interface related with UHPC was in combination with LWC (Banta 2005), HPC (Crane 2010), and NSC (Jang et al. 2017). Jang et al. (2017) conducted push-off tests in NSC-UHPC and UHPC-UHPC composites focusing on construction joints. The researchers did not investigate cases with interface reinforcement. Banta (2005) and Crane (2010) mostly focused on behavior of the interface reinforcement with a smooth interface. Thus, behavior of interface reinforcement in NSC-UHPC composites with roughened interfaces needs to be studied in detail. In addition, there are limited flexural tests carried out for NSC-UHPC composites, especially with the incorporation of UHPC as filler material between the precast elements. Therefore, a detailed experimental program including push-off tests and four-point bending tests was developed and presented in this paper to further understand the interface behavior of NSC-UHPC composites.

Sharma et al. (2019) used partial data from this study combined with data in literature to perform reliability analysis on current design equations, without much discussion on testing and observed behavior. Ronanki et al. (2019) used test results from one set of push-off specimens and composite beam tests to validate their detailed 3D finite element models for analysis of a hybrid precast bridge girder with a NSC-UHPC interface. This paper presents the details of experimental results, including interface reinforcement behavior and dilation at the interface, of all test specimens. The scope of this paper is to evaluate the interface shear behavior at NSC-UHPC interface and current design provisions based on the experimental results.

Experimental Program

This section presents details of an experimental testing program. The experimental program consisted of 10 NSC-UHPC push-off specimens and four NSC-UHPC composite beam specimens.

Push-off Test Specimens

Composite push-off specimens consisting of NSC and UHPC were built to study the impact of surface roughness and interface shear reinforcement on the interface shear capacity. To create consistent and repeatable interface roughness across different specimens, two textures, namely, Wisla and Parana from Reckli formliners, were selected. Fig. 1 provides details of the formliners used in push-off specimens.

The dimensions of NSC and UHPC parts of the push-off specimens were $305 \times 229 \times 216$ mm ($12 \times 9 \times 8.5$ in.) and $254 \times 178 \times 140$ mm ($10 \times 7 \times 5.5$ in.), respectively. The NSC-UHPC interface area of the specimen was 40,645 mm^2 (63 in.^{2}). Different quantities of two-legged #3 bars [$d_b = 9.5$ mm (0.375 in.); $d_b =$ diameter of

rebar] were used as interface shear reinforcement. Four 16 mm (0.63 in.) diameter high-strength threaded bars were used as longitudinal reinforcement in the NSC portion, while two 16 mm diameter (0.63 in.) high-strength threaded bars were used as longitudinal reinforcement in the UHPC portion. The longitudinal bars were left protruded out of the UHPC block and the NSC substrate to bolt a steel W section for testing purposes. Standard 9.5 mm (3/8 in.) long foil strain gauges were placed on the interface reinforcements to monitor strains at the NSC-UHPC interface, NSC portion, and UHPC portion. The strain gauges were placed as close as practically possible to the interface (centerline of gauge was at 10 mm from the interface). The strain gauges in the NSC portion were installed at 60 mm (2.4 in.) from the interface. The strain gauges in the UHPC portion were installed at 25 mm (1 in.) from the interface. The locations of the strain gauges are shown in Fig. 2(a). The formwork for the specimens were made of plywood. A standard 34.5 MPa (5 ksi) NSC mix from a local ready-mix concrete producer was used to cast the NSC substrates. The concrete mix contained 15.9 mm (0.625 in.) maximum aggregate size and had 175 mm (7 in.) slump. Immediately after casting, formliners were placed on top of the NSC surface to produce the desired texture across the interface as shown in Fig. 2(b). A smooth texture was created by finishing the surface using a standard wood trowel to match construction practices. The formliners were removed after 24 hours of casting. The formworks were demolded after three days of casting. The NSC substrates were covered using wet burlaps for the first week. The specimens were then air cured in ambient laboratory conditions [23°C and 50% relative humidity (RH)] for the next three weeks. UHPC was mixed as per the manufacturer's instructions using a standard mortarman 750 mixer. The NSC substrates were kept wet for 24 hours prior to pouring of UHPC. This was done to obtain a saturated surface dry (SSD) condition at the interface. UHPC was poured into the forms from one end of the specimen, allowing free flow of UHPC to obtain uniform distribution of fibers along the interface. The specimens were covered with plastic shrink-wrap and a tarp for three days after casting to prevent moisture loss from UHPC. The formworks were demolded after three days. The specimens were air cured in ambient laboratory conditions (23°C and 50% RH) for more than 28 days.

Table 2 lists a nomenclature and additional details of push-off specimens. The first two letters of the specimen nomenclature show the type of concrete used in the specimen: N = NSC and U = UHPC. Next set of letters describe the type of interface preparation: SM = smooth; WI = Wisla; and PI = Parana. The last digit

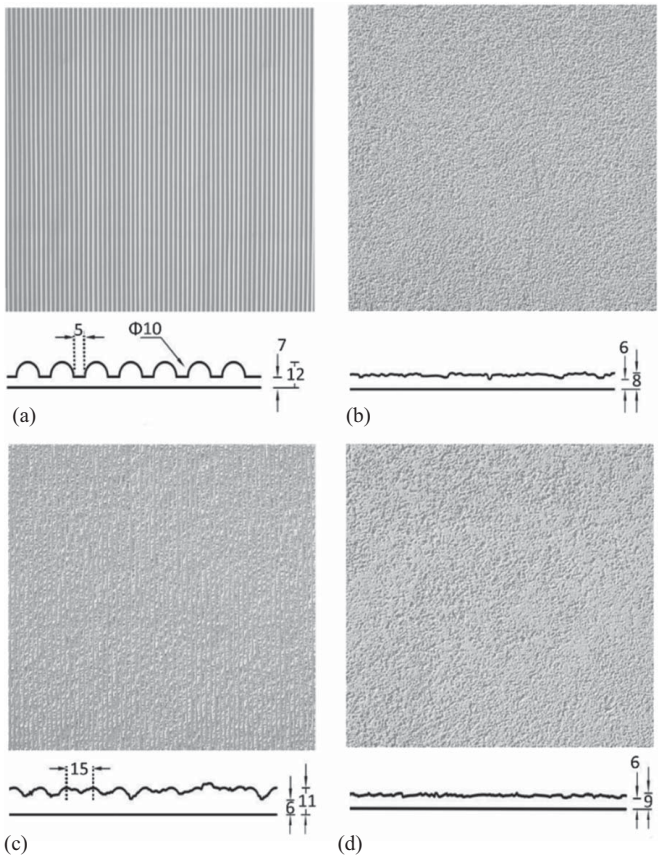

Fig. 1. Surface texture type and roughness depth used in NSC-UHPC interface in push-off and composite beam specimens: (a) Wisla (5.08 mm); (b) Parana (2.03 mm); (c) Indus (4.83 mm); and (d) Rio bravo (2.80 mm); 25.4 mm = 1 in.

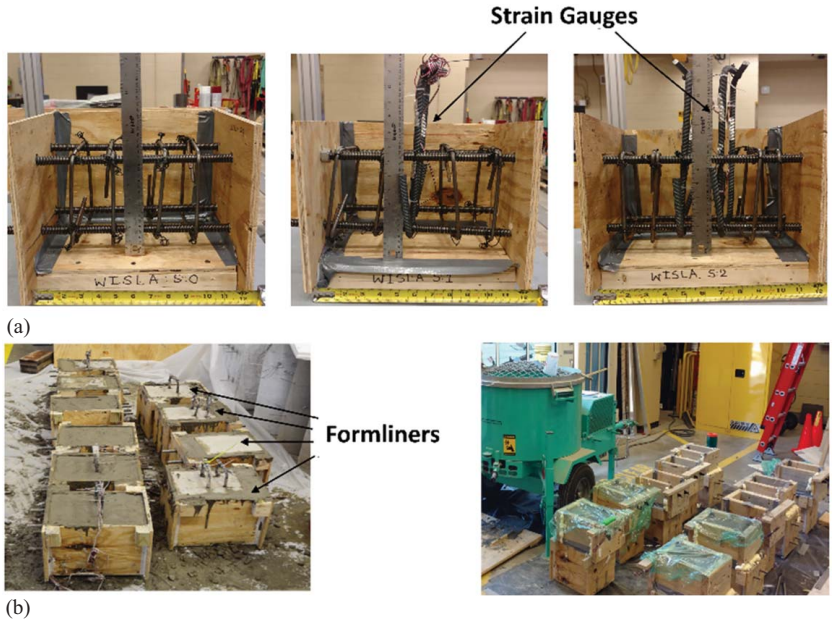

Fig. 2. Specimen fabrication of push-off specimens: (a) formwork and reinforcement cage; and (b) NSC-UHPC casting.

Table 2. Details of push-off specimens

Specimen ID	Shear interface texture	Interface roughness depth mm (in.)	Interface area mm^2 (in^2)	Area of interface shear reinforcement mm^2 (in^2)
N-U-SM-0-A	Smooth	0.00 (0.0)	40,129 (62.20)	0
N-U-SM-0-B	Smooth	0.00 (0.0)	41,581 (64.45)	0
N-U-PI-0	Parana	2.03 (0.08)	40,284 (62.44)	0
N-U-WI-0	Wisla	5.08 (0.20)	41,084 (63.68)	0
N-U-SM-1-A	Smooth	0.00 (0.00)	41,129 (63.75)	142 (0.22)
N-U-SM-1-B	Smooth	0.00 (0.00)	42,678 (66.15)	142 (0.22)
N-U-PI-1	Parana	2.03 (0.08)	41,458 (64.26)	142 (0.22)
N-U-WI-1	Wisla	5.08 (0.20)	39,632 (61.43)	142 (0.22)
N-U-PI-2	Parana	2.03 (0.08)	43,671 (67.69)	284 (0.44)
N-U-WI-2	Wisla	5.08 (0.20)	40,522 (62.81)	284 (0.44)

Table 3. Details of composite beam specimens

Serial no.	Specimen ID	Horizontal interface texture	Horizontal texture roughness mm (in.)	Vertical interface texture	Clear cover mm (in.)
1	N-U-B1-WI	Wisla	5.08 (0.20)	Wisla	69.85 (2.75)
2	N-U-B2-IN	Indus	4.83 (0.19)	Wisla	63.5 (2.50)
3	N-U-B3-RB	Rio Bravo	2.80 (0.11)	Wisla	57.15 (2.25)
4	N-U-B4-RB	Rio Bravo	2.80 (0.11)	Wisla	44.45 (1.75)

denotes the number of two-legged #3 (US size) shear reinforcement passing the interface. Suffix "A" and "B" are used to distinguish two specimens having the same interface preparation and reinforcement area across the interface.

Composite Beam Specimens

Four NSC-UHPC composite beams were constructed to study interface shear capacity at the horizontal interface under flexural loading. The NSC substrate was designed to mimic typical bridge deck structures that are repaired by application of thin layers of UHPC overlay. The NSC substrate was provided with minimal longitudinal tension reinforcement using two #4 US-size bars [d_bc12.7 mm (0.5 in.)]. The longitudinal bars had different clear cover (Table 3) and were spliced at the center with a total splice length of 152 mm (6 in.) to serve the purpose of a separate study. Shear reinforcement was not provided in the NSC substrate to represent typical bridge decks. Three textures, namely, Wisla, Indus, and Rio Bravo from Reckli formliners, were selected to create interface roughness for composite beam specimens. Fig. 1 provides details of the formliners used in composite beam specimens. Table 3 lists the combination of interface texture across horizontal and vertical interface.

The NSC substrate in the NSC-UHPC composite beam specimen was 813 mm (32 in.) in length, 152 mm (6 in.) wide, and 178 mm (7 in.) deep on either side of the central UHPC block. The UHPC block was 203 mm long (8 in.) and a similar cross section to the NSC section. The formworks for the NSC part were built using plywood and the spaces for the central UHPC block were created with styrofoam as shown in Fig. 3(a). Formliners of desired texture were attached at the vertical interface adjacent to the styrofoam and at the top of the NSC substrate. These specimens were poured at the same time as the push-off specimens using the same normal concrete mix. Both the formliners and the formwork were removed three days after pouring. The NSC part was covered with wet burlaps for seven days after pouring. The specimens were then air cured in ambient laboratory conditions (23°C and 50% RH) for the next three weeks. After the NSC part was cured, UHPC was poured in the central block and was air cured in ambient laboratory conditions for more than 28 days. An additional formwork was built on top of the NSC substrate for pouring of the second layer of UHPC with an overlay

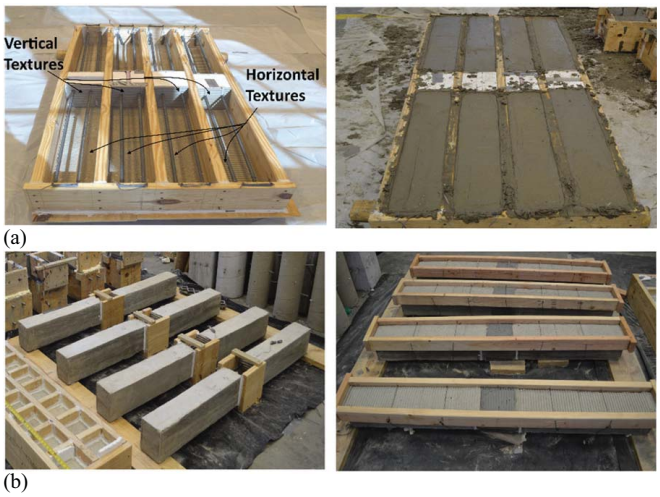

Fig. 3. Specimen fabrication of composite beam specimens: (a) formwork and pouring of NSC; and (b) formworks for pouring UHPC at mid-span and overlay.

thickness of 32 mm (1.25 in.). The NSC substrate was kept wet for 24 hours prior to UHPC pour. This was done to obtain SSD condition at the interface. After each pour, the UHPC part was covered with a plastic shrink-wrap and a tarp to prevent loss of moisture until the specimens were demolded. Formworks for UHPC were demolded after three days. The UHPC overlay layer was air cured for more than 28 days in ambient laboratory conditions.

Test Setup

Push-off Test

The push-off test specimens were tested at the Large-Scale Structures Laboratory at the University of Alabama using the test setup shown in Fig. 4(a). The specimens were loaded using a manually controlled, 890 kN (200 kip) capacity hydraulic jack. The NSC-UHPC push-off specimen was bolted to a steel W beam at the top and bottom using the embedded threaded rods. A laser level was used to align the centerline of the loading plate and

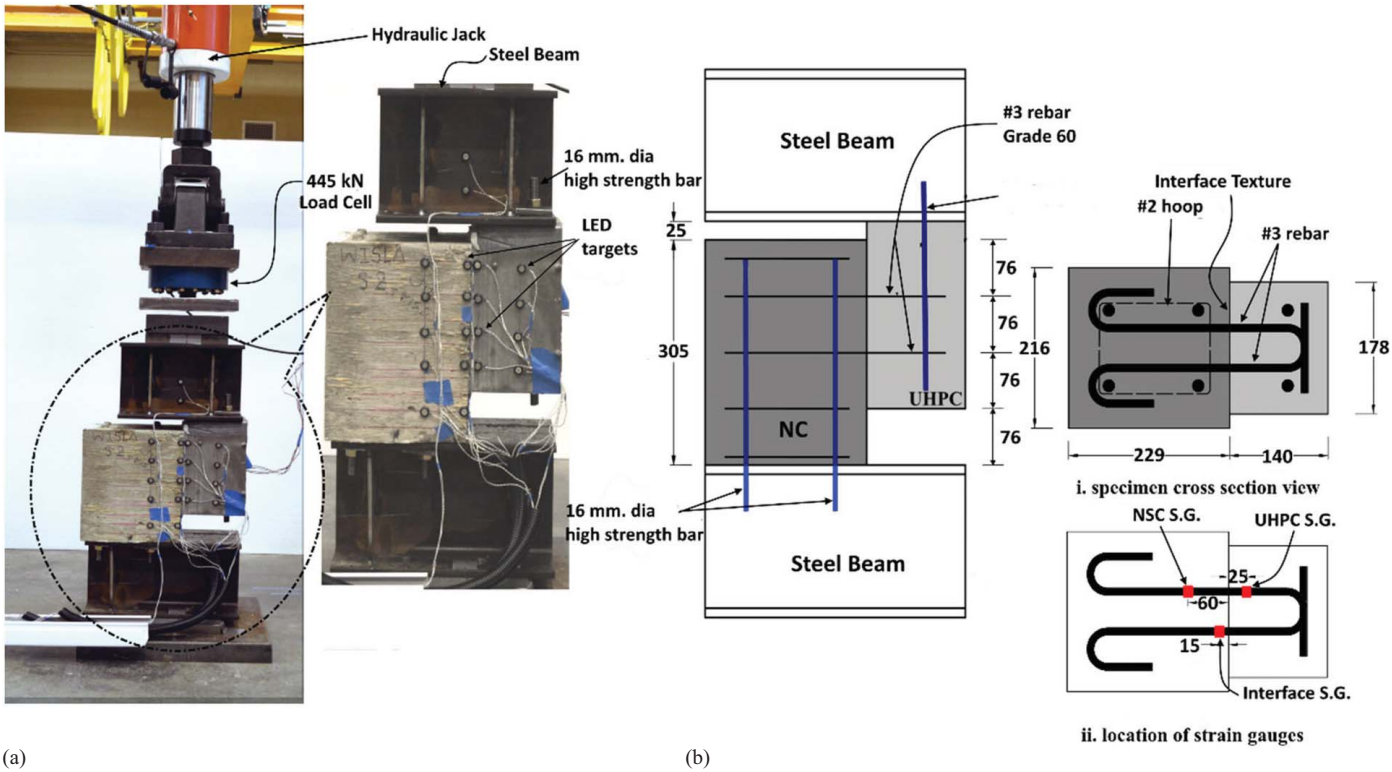

Fig. 4. Test setup and specimen details for push-off specimen: (a) test setup of push-off specimen; and (b) specimen dimension and location of strain gauges (25.4 mm = 1 in.).

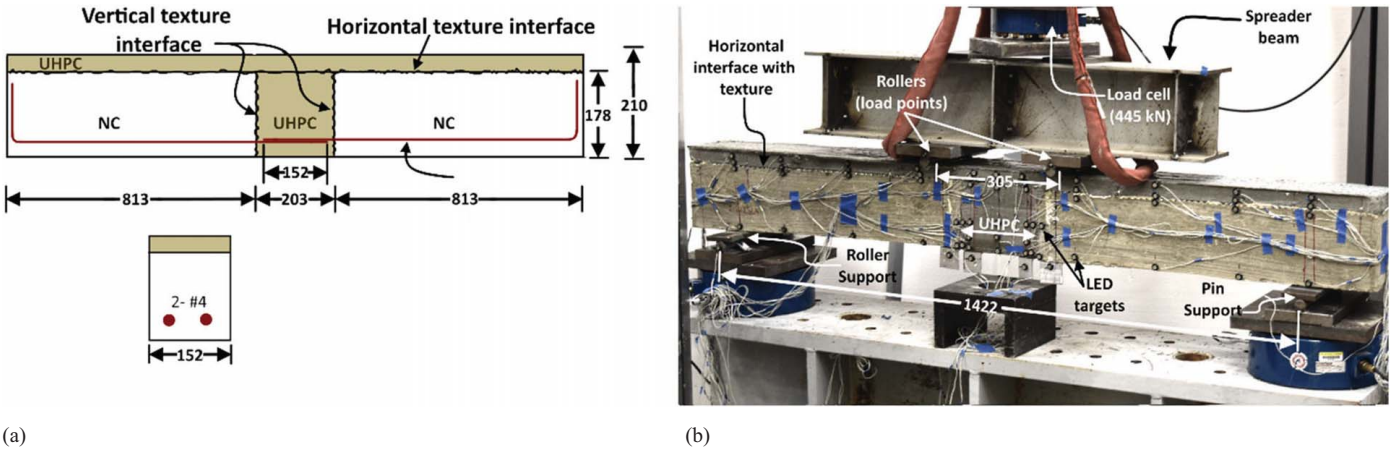

Fig. 5. Test setup and specimen details for composite beam specimen: (a) details of NSC-UHPC; and (b) test setup and instrumentation (25.4 mm=1 in.).

the interface of the composite specimen. An NDI Optotrak system, a 3D noncontact displacement measurement system, was used to measure interface slip and dilation at the interface. Typically, four pairs of light emitting diodes (LEDs) were equally spaced along the NSC-UHPC interface as shown in Fig. 4(a). The Optotrak system recorded 3D coordinates of the LEDs at a frequency of 10 Hz. Data from strain gauges on the interface reinforcements and the load cells were recorded using a national instruments (NI) data acquisition (DAQ) system at the same frequency as the Optotrak system. Loading was applied monotonically in increments of 22.24 kN (5 kip) and specimens were inspected for damage at every increment. Specimens with interface shear reinforcement were loaded until at least one of the interface reinforcements fractured (Fig. 5).

Composite Beam Test

The composite beam specimens were subjected to four-point bending using an 890 kN (200 kip) capacity, manually operated hydraulic jack. The composite beam was simply supported over 1,422 mm (56 in.). Two load cells of 890 kN (200 kip) capacity each were placed at the supports of the beam to measure support reactions as shown in Fig. 6(b). The applied load was measured using a 445 kN (100 kip) capacity load cell attached to the hydraulic jack. Data from the load cells were recorded using a NI DAQ system at 10 Hz frequency. The NDI Optotrak system was used to capture displacement and slip at the interface and calculate strain distribution in the UHPC and NSC layers. The distribution of NDI LEDs is shown in Fig. 6(b). Data from the top and bottom LEDs across the height of the beam were used to

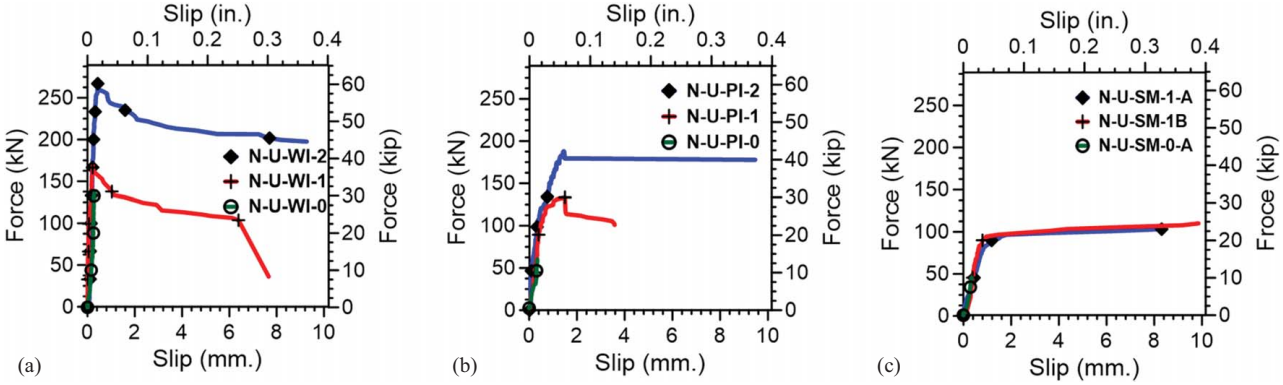

Fig. 6. Force versus slip relationship across varying interface roughness: (a) Wisla; (b) Parana; and (c) smooth. Slip value limited to 10.16 mm (0.4 in.).

Table 4. Material properties

	UHPC compressive strength MPa (ksi)		NSC compressive strength MPa (ksi)	
Specimen	28 days	Test day	28 days	Test day
N-U-SM-0-A	123.23 (17.88)	143.83 (20.86)	45.02 (6.53)	48.26 (7.00)
N-U-SM-0-B	123.23 (17.88)	143.83 (20.86)	45.02 (6.53)	48.26 (7.00)
N-U-PI-0	123.23 (17.88)	145.67 (21.13)	45.02 (6.53)	46.75 (6.78)
N-U-WI-0	123.23 (17.88)	145.67 (21.13)	45.02 (6.53)	46.75 (6.78)
N-U-SM-1-A	123.23 (17.88)	140.03 (20.31)	45.02 (6.53)	47.99 (6.96)
N-U-SM-1-B	123.23 (17.88)	140.03 (20.31)	45.02 (6.53)	47.99 (6.96)
N-U-PI-1	123.23 (17.88)	139.83 (20.28)	45.02 (6.53)	46.68 (6.77)
N-U-WI-1	123.23 (17.88)	139.83 (20.28)	45.02 (6.53)	48.81 (7.08)
N-U-PI-2	123.23 (17.88)	146.72 (21.27)	45.02 (6.53)	47.51 (6.89)
N-U-WI-2	123.23 (17.88)	139.83 (20.28)	45.02 (6.53)	46.61 (6.76)
N-U-B1-WI	123.23 (17.88)[a] 134.59 (19.52)[b]	143.54 (20.81) 151.83 (22.02)	45.02 (6.53)	47.57 (6.90)
N-U-B2-IN	123.23 (17.88)[a] 134.59 (19.52)[b]	146.73 (21.28) 149.21 (21.64)	45.02 (6.53)	48.13 (6.98)
N-U-B3-RB	123.23 (17.88)[a] 134.59 (19.52)[b]	140.66 (20.40) 148.73 (21.57)	45.02 (6.53)	46.61 (6.76)
N-U-B4-RB	123.23 (17.88)[a] 134.59 (19.52)[b]	144.52 (20.96) 150.30 (21.80)	45.02 (6.53)	46.26 (6.71)

[a]Properties of mid-section UHPC pour of composite beams.
[b]Properties of overlay UHPC pour of composite beams; UHPC compressive strengths are obtained from 50 mm (2 in.) cubes.

calculate maximum compressive and tensile strains in the specimen. Data from the middle two LEDs were used to calculate interface slip and corresponding strain across the interface. Two point loads were applied at 152.5 mm (6 in.) to the left and right of the center of the beam through a spreader beam. Loading was applied monotonically in increments of 8.9 kN (2 kip), up to failure of the specimen.

Results and Discussion

Material Tests

The average 28 days and test day compressive strengths of UHPC and NSC were obtained from 50.8 mm (2 in.) cube and standard 101.6 × 152.4 mm (4 × 6 in.) cylinder testing, respectively. The UHPC cube strengths were modified with a factor of 0.96 to obtain the equivalent UHPC cylinder compressive strength (Graybeal and Davis 2008). The compression tests on NSC cylinders were carried out using the ASTM C39 procedure (ASTM 2020). The measured compressive strength values for UHPC and NSC for all test specimens are listed in Table 4. The compressive strength of UHPC at the time of testing varied from 140 MPa to 151.8 MPa (20.31 ksi to 22.02 ksi). The tensile testing of #3 [$d_b = 9.5$ mm (0.375 in.)] mild steel reinforcement was carried out using the ASTM E8 procedure (ASTM 2013). The yield stress and yield strain values obtained from the tensile testing were 431.27 MPa (62.55 ksi) and 0.00193 mm/mm (in./in.), respectively.

Table 5. Results from push-off tests

Specimen ID no.	Cracking load[a] kN (kip)	Peak load kN (kip)	Slip[b] mm. (in.)	Crack width[b] mm. (in.)	Strain in interface reinforcement[b]	Shear stress MPa (ksi)	Failure mode
N-U-SM-0-A	N/A	44.97 (10.11)	0.33 (0.012)	N/A	N/A	1.10 (0.16)	I
N-U-PI-0	N/A	62.23 (13.99)	0.33 (0.012)	1.52 (0.06)	N/A	1.52 (0.22)	I
N-U-WI-0	N/A	137.63 (30.94)	0.28 (0.011)	0.05 (0.002)	N/A	3.38 (0.49)	I
N-U-SM-1-A[c]	82.55 (18.56)	82.60 (18.57)	0.940 (0.037)	0.05 (0.002)	0.0042	2.00 (0.29)	I
N-U-SM-1-B[c]	7.11 (1.60)	93.41 (21.00)	0.940 (0.037)	0.38 (0.015)	0.0100[d]	2.21 (0.32)	I
N-U-PI-1	98.17 (22.07)	134.38 (30.21)	1.47 (0.06)	0.61 (0.024)	0.0130	3.24 (0.47)	I
N-U-WI-1	153.2 (34.44)	169.66 (38.14)	0.22 (0.01)	0.02 (0.001)	0.0023	4.27 (0.62)	I
N-U-PI-2[c]	99.02 (22.26)	187.76 (42.21)	1.45 (0.057)	0.41 (0.016)	0.0091	4.29 (0.62)	I
N-U-WI-2	256.17 (57.59)	269.34 (60.55)	0.43 (0.017)	0.09 (0.004)	0.0018	6.62 (0.96)	I

Note: I = failure at interface.
[a]Measured at approximately 0.025–0.050 mm. (0.001–0.002 in.) crack width at location of interface reinforcement. In case of specimens with two interface reinforcements, the cracking load corresponds to the crack width at either of rebar locations exceeding 0.025–0.050 mm.
[b]Measured at peak load.
[c]Peak load is taken as load reached at the end of first slope as seen in Figs. 6 and 7 after which the specimen slipped rapidly and continued to gain strength.
[d]Maximum recorded reading of strain gauge at 89 kN (20.07 k).

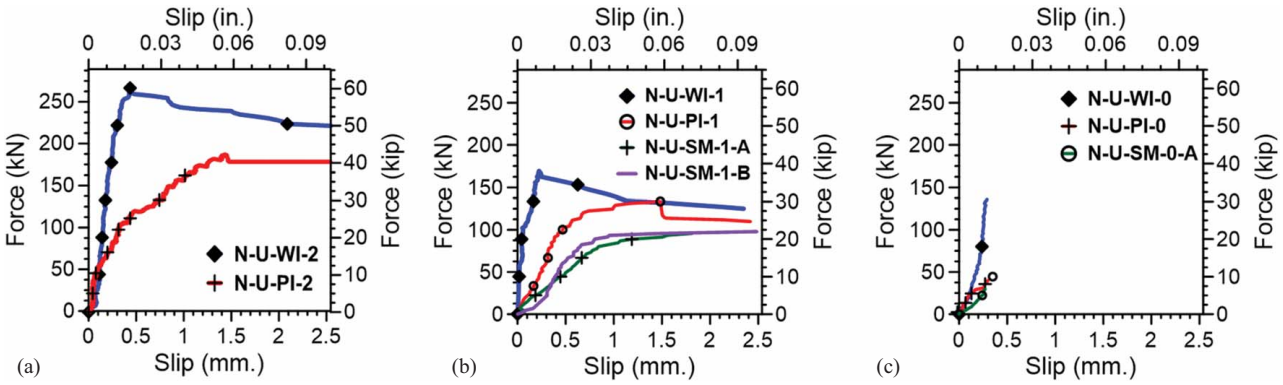

Fig. 7. Force versus slip relationship across varying area of interface reinforcement: (a) two two-legged #3 stirrups; (b) one two-legged #3 stirrups; and (c) no stirrups. Slip value limited to 2.54 mm (0.1 in.).

Push-off Test

Ten specimens with different surface textures and interface reinforcement ratio were tested under direct shear. The results from the push-off tests are presented in terms of load, slip and dilation in the interface, failure mode, and strain in the interface reinforcement (Table 5). Figs. 6 and 7 show the measured force versus slip relationship for specimens with different interface textures and reinforcement ratios, respectively. The plots were limited to a vertical slip value of 10.16 mm (0.4 in.) in Fig. 6 and 2.54 mm (0.1 in.) in Fig. 7 for better presentation of data. One specimen (N-U-SM-0-B) failed prematurely due to accidental loading before the data collection was started and was excluded from Figs. 6 and 7 and Table 5. The specimens with higher interface roughness such as the Parana interface [PI: 2 mm (0.08 in.)] and the Wisla interface [WI: 5 mm (0.2 in.)] performed better than the smooth interface (SM) specimens. Specimens with the same surface roughness but with increased interface reinforcement resisted higher shear. Specimens with the Wisla (WI) interface had the highest shear strength.

All specimens had a linear force versus slip relationship until cracking along the interface commenced. The resistance to this shear is provided by cohesion between NSC and UHPC particles. In the case of PI specimens, the cracking load is similar at different reinforcement ratios, whereas for WI specimens, the cracking load is higher for the specimen with a higher interface reinforcement ratio. The cracking load is defined as the load corresponding to interface crack widths (dilation) of 0.025–0.05 mm (0.001–0.002 in.) at the interface reinforcement location. The interface reinforcement in N-U-PI-1 and N-U-PI-2 specimens was strained in tension near the cracking load, whereas in case of N-U-WI-1 and N-U-WI-2, the interface reinforcement was strained in tension before the cracking load. For example, the tensile strain in the interface reinforcement in specimens N-U-PI-1 and N-U-PI-2 was first recorded at 89.38 kN (20.09 k) and 98.07 kN (22.05 k), respectively, which are within 10% of their corresponding cracking loads. Similarly, in specimens N-U-WI-1 and N-U-WI-2, the rebars were strained at 89.14 kN (20.03 k) and 133.89 kN (30.10 k), which are around 55% of corresponding cracking load. Based on the observation, the deeper texture causes the interface reinforcement to engage prior to noticeable (visible) interface cracking, which can explain the higher cracking load for deeper textures with more reinforcement.

The interface crack widened with application of additional shear load as shown in Fig. 8. The crack opening for smooth specimens, N-U-SM-0-A and N-U-PI-0, was too small to be accurately measured, and thus is not shown in the figure. The interface reinforcements experienced higher strain values with opening of the interface crack and provided normal clamping force across the interface. The force versus slip relationship is quasi-linear between the initial cracking and the peak shear capacity of the specimen. However, in specimens having smooth interface texture, significant slip was observed immediately after opening of the interface crack. As the coefficient of friction for smooth surfaces are relatively lower, the shear friction acting along the interface is

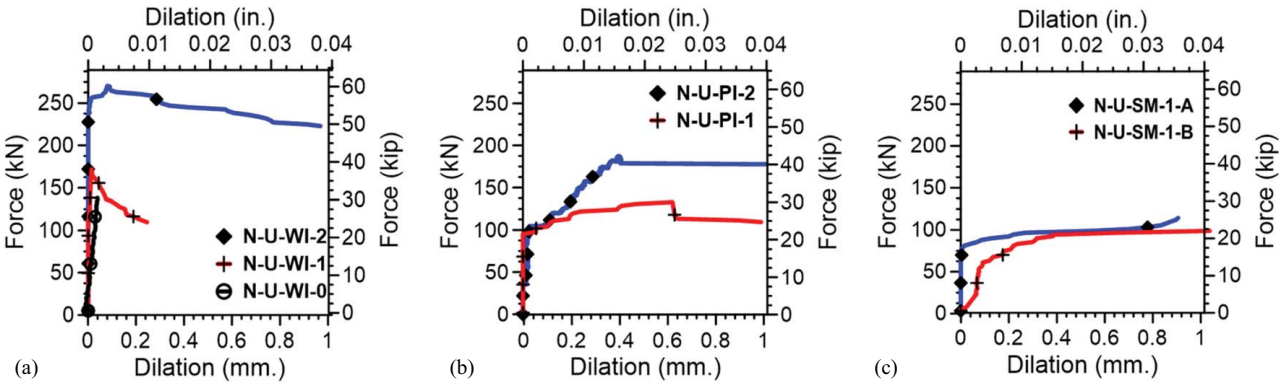

Fig. 8. Force versus dilation relationship across varying interface roughness: (a) Wisla; (b) Parana; and (c) smooth.

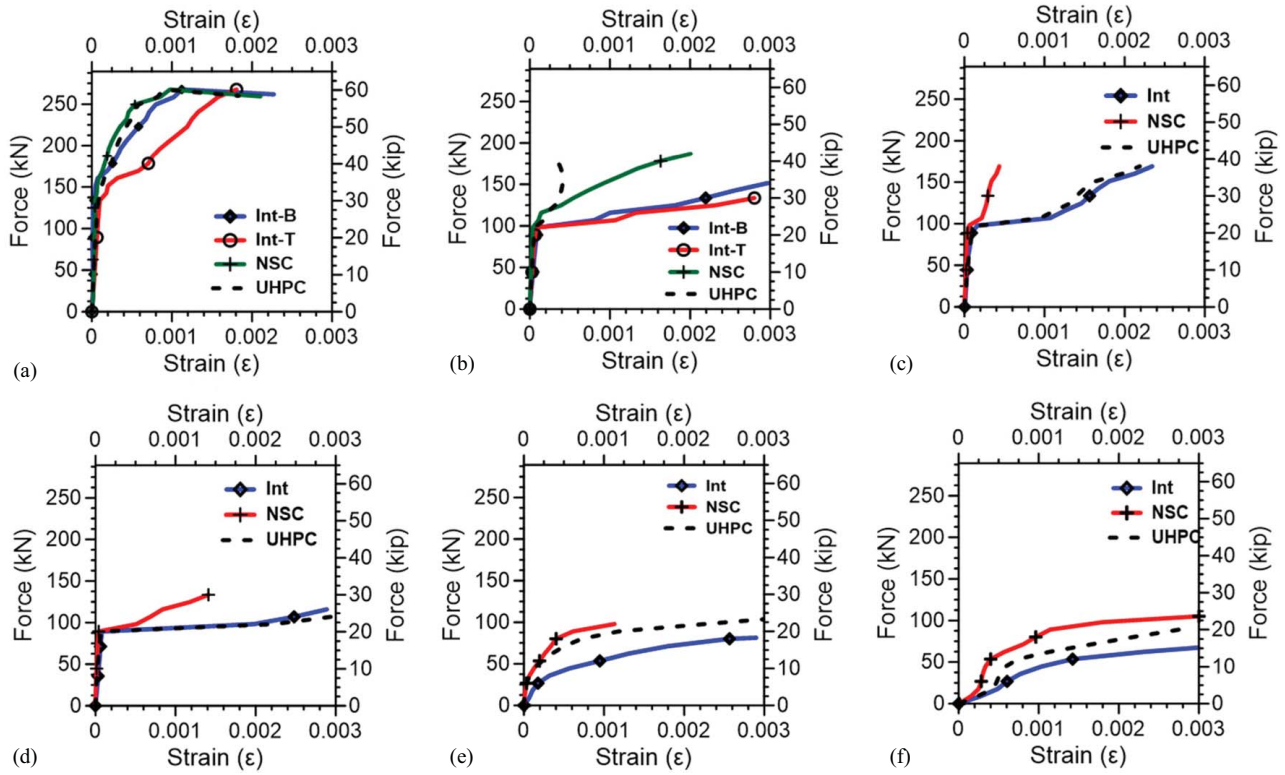

Fig. 9. Force versus strain relationship across varying interface texture and reinforcement ratio: (a) N-U-WI-2; (b) N-U-PI-2; (c) N-U-WI-1; (d) N-U-PI-1; (e) N-U-SM-1-A; and (f) N-U-SM-1-B. Strain values limited to 0.003.

also low for similar clamping forces. As a result, specimens with lower interface roughness underwent higher slip as shear load increased [Figs. 7(a and b)].

For specimens having interface reinforcement, rebar strain measurements at the interface, in NSC substrate and in UHPC are plotted against the applied load in Fig. 9. The strain values at the peak load varied for specimens with different interface textures. The interface rebar of specimen N-U-WI-2 had strain values of 1,800 micro strain at the peak load while the interface bars of specimen N-U-PI-2 were past yield at the peak capacity. Similarly, the interface bars of specimen N-U-WI-1 had strain values around 2,300 micro strain while the interface bars of specimen N-U-PI-1 and N-U-SM-1A and N-U-SM-1B were well past yield. The specimens with WI texture [texture depth = 5 mm (0.2 in.)] reached peak shear load at lower slip and the strain measured in the interface reinforcement was lower when compared with the specimen with PI texture [texture depth = 2 mm (0.08 in.)] and SM texture (texture depth = 0 mm.). It should also be noted that the increment in peak capacity of N-U-WI-2 from N-U-WI-1 was 60%, while the increment in peak capacity of N-U-PI-2 from N-U-PI-1 was 40%. Based on the experimental results, the shear capacity of the specimens did not increase by the same ratio as that of interface reinforcement. Additional tests are required to develop an accurate relationship between reinforcement ratio, roughness, and interface shear capacity.

After reaching the peak load, the specimens with WI texture and interface reinforcement began to slip, and the crack width increased considerably. The specimen had residual shear capacity as the bars were close to yield stress at the peak shear load. The specimen finally failed due to rupture of interface reinforcement. In specimens N-U-WI-2 and N-U-WI-1, the NSC substrate

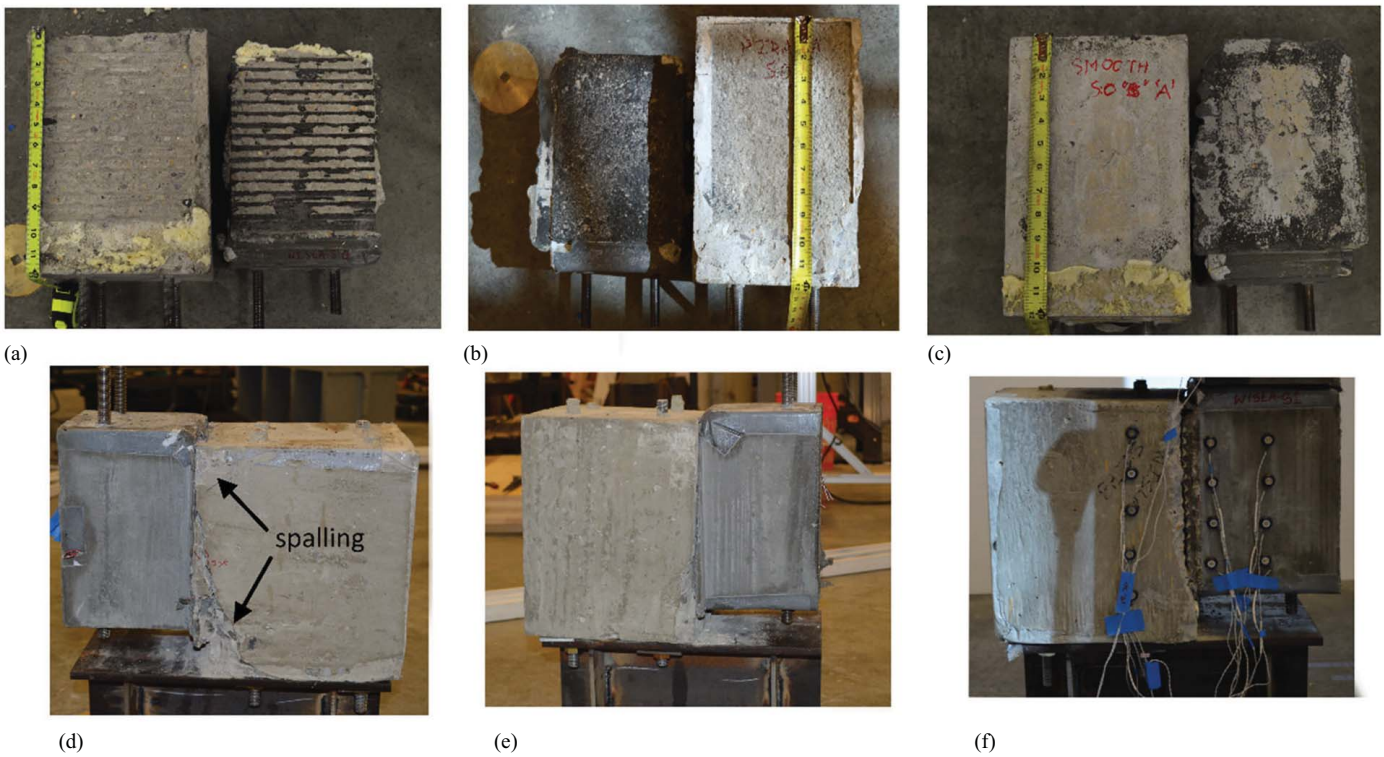

(a) (b) (c) (d) (e) (f)

Fig. 10. Photos of interface after failure of push-off specimens: (a) N-U-WI-0; (b) N-U-PI-0; (c) N-U-SM-0-A; (d) N-U-WI-2; (e) N-U-PI-2; and (f) N-U-WI-1.

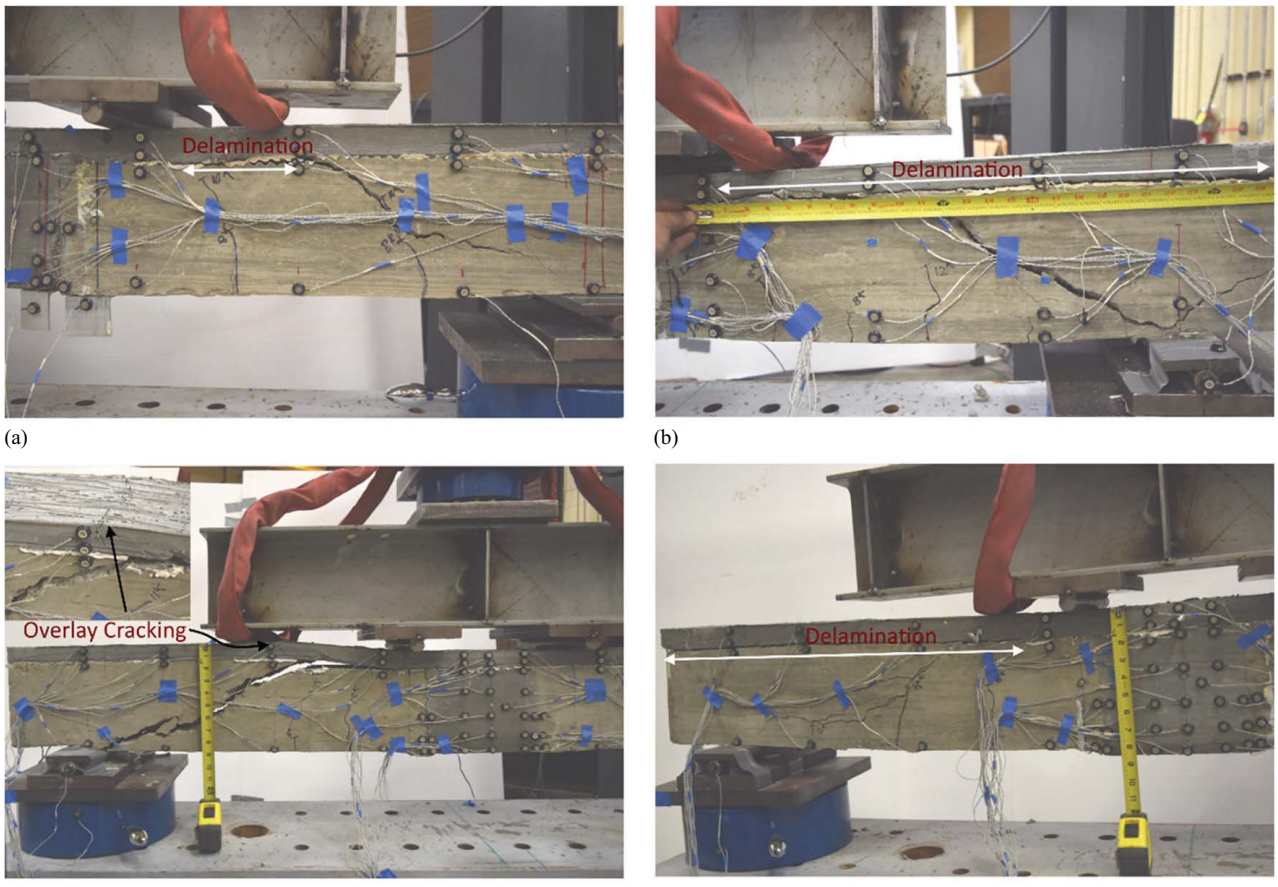

(a) (b) (c) (d)

Fig. 11. Interface failure mode at NSC-UHPC in composite beam specimens: (a) N-U-B1-WI; (b) N-U-B2-IN; (c) N-U-B3-RB; and (d) N-U-B4-RB.

spalled at the interface as shown in Figs. 10(d and f). In specimens with low interface roughness, that is, with PI and SM textures, the postpeak behavior was different. The N-U-PI-2 specimen experienced considerable slip but kept resisting shear nearly equal to the peak load. The specimen continued resisting shear due to strain hardening behavior and possible dowel action of the interface reinforcement and failed with rupture of the bars. In the case of specimen N-U-PI-2, no major spalling at the interface was observed as seen in Fig. 10(e). Specimen N-U-PI-1 exhibited a slight drop in shear resistance and eventually failed due to rupture of bars. In N-U-SM-1-A and N-U-SM-1-B, the specimens started slipping rapidly after reaching peak load and failed after rupture of the interface bars. The peak shear resistance and corresponding behavior up to failure were primarily dictated by yielding and possible dowel behavior of the interface reinforcement due to high slip values. These specimens lacked functional ductility and residual shear capacity. The specimens without any interface reinforcement (N-U-WI-0, N-U-PI-0, N-U-SM-0-A, and N-U-SM-0-B) failed in a brittle manner immediately after reaching peak load as shown in Figs. 11(a–c).

Composite Beam Flexural Test

During the test, all the specimens started developing flexural cracks around 11.1 kN (2.5 kips) point load and ultimately failed due to shear in the NSC substrate. The specimens also exhibited several flexural cracks at failure. The interface slip was negligible until significant shear cracking was observed in the NSC substrate. Once shear cracking in normal concrete was predominant, the NSC-UHPC interface experienced delamination. In specimen N-U-B1-WI, where the horizontal interface roughness was created by 5.08 mm (0.2 in.) deep grooves, the delamination was limited to the zone between shear crack and the point load in the interface. The remaining length of the interface was intact as shown in Fig. 11(a). In specimen N-U-B2-IN, where the interface texture roughness was 4.8 mm (0.19 in.), the delamination extended all the way on one side (from the location of point load to end of the beam). The delamination was sudden and occurred as soon as the specimen failed in shear [Fig. 11(b)]. In specimen N-U-B3-RB, where the interface roughness was 2.8 mm (0.11 in.), the delamination was limited between shear crack and the point load in interface. Some cracking and discontinuity in UHPC overlay were observed [Fig. 11(c)]. In specimen N-U-B4-RB, the delamination occurred all the way from the point load location to the end of the beam on one side [Fig. 11(d)]. Based on the experimental observations, N-U-B1-WI experienced the least damage at the horizontal interface. There was no delamination except at a small zone between the shear cracks and the point load. These effects of shear cracking on the nature of UHPC interface failure in flexural specimens with insufficient deficient shear capacities warrants further study.

Fig. 12(a) shows strain distribution of the composite beam specimens close to failure. The strain measurements were calculated based on the deformation of LEDs across the vertical NSC-UHPC interface and the corresponding UHPC overlay. The strain distribution close to peak load is nearly linear for all specimens that show excellent composite behavior under flexure. Fig. 12(b) shows load versus displacement relationship for the composite specimens. The relationship was nearly linear up to failure, after which displacement suddenly increased due to shear failure.

Since the composite specimens did not experience slipping at the interface before failure, the interface shear capacity calculated using simple beam theory can provide lower bound for shear capacity of the interfaces. The horizontal shear stress across the interface can be calculated by dividing the shear force at that section with effective depth and width of the section (ACI 318-14, ACI 2014). The calculated interface shear stress values are listed in Table 6.

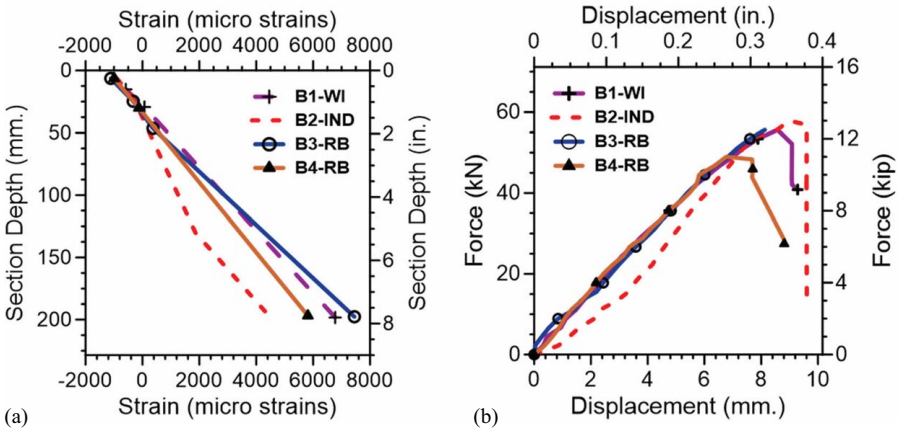

Fig. 12. Strain distribution and force-displacement response for NSC-UHPC composite beams: (a) section depth versus strain; and (b) load versus displacement.

Table 6. Results from composite beam tests

Specimen ID no.	Avg. thickness overlay mm (in.)	Avg. width mm (in.)	Effective depth (d_e) mm (in.)	Load[a] kN (kip)	Load[b] kN (kip)	Load[c] kN (kip)	Interface shear stress MPa (ksi)	Failure mode
N-U-B1-WI	35.6 (1.40)	152.4 (6.0)	137.21 (5.40)	55.60 (12.50)	27.05 (6.08)	28.55 (6.42)	1.33 (0.19)	NCVS
N-U-B2-IN	33.0 (1.29)	149.4 (5.88)	140.96 (5.55)	57.82 (13.00)	29.30 (6.59)	28.52 (6.41)	1.37 (0.20)	NCVS
N-U-B3-RB	32.3 (1.27)	152.4 (6.0)	146.61 (5.77)	55.60 (12.50)	28.96 (6.51)	26.64 (5.99)	1.24 (0.18)	NCVS
N-U-B4-RB	38.1 (1.50)	152.4 (6.0)	165.11 (6.50)	48.97 (11.01)	24.95 (5.61)	24.02 (5.40)	0.97 (0.14)	NCVS

Note: NCVS = normal concrete vertical shear; Load[a] = total force applied by hydraulic jack to the spreader beam; Load[b] = force recorded on load cell placed at the left support of the beam referring to Fig. 6(b); and Load[c] = force recorded on load cell placed at right support of the beam referring to Fig. 5(b).

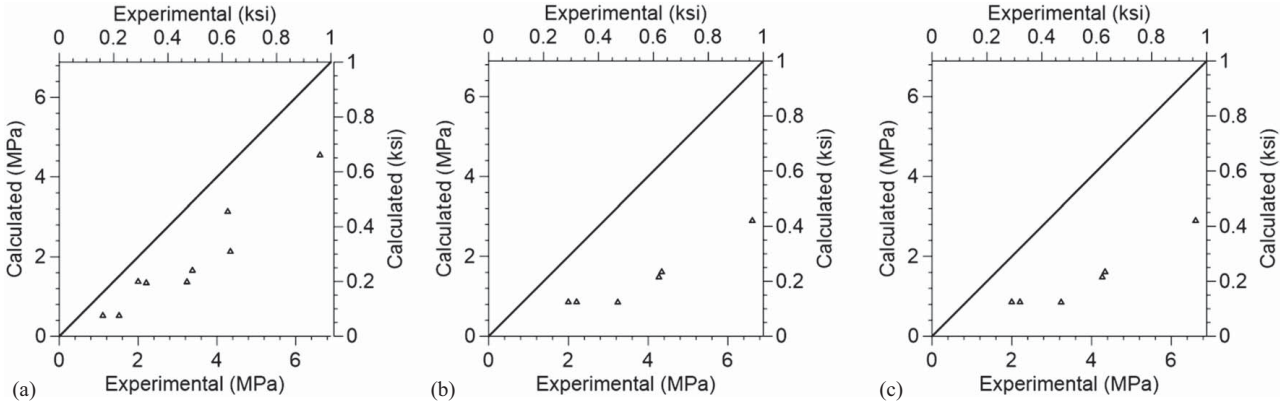

Fig. 13. Comparison of calculated and experimental results: (a) AASHTO; (b) ACI; and (c) PCI.

Owing to shear failure, specimen N-U-B1-WI was subjected to a horizontal shear stress of 1.33 MPa (0.19 ksi), which is just 39% of the shear capacity obtained from the push-off test of the specimen with the same interface texture (N-U-WI-0). The horizontal shear stress values obtained from the experiments at failure of the substrates (Table 6) were higher than the AASHTO (2017) recommended value of 0.52 MPa (75 psi) for roughness depth lower than 6.4 mm (0.25 in.) (Table 1). During testing, no damage was observed in the UHPC overlay itself. The average overlay thickness across the test specimens was 34.75 mm (1.37 in.). Based on the experimental results, UHPC overlay thickness of 35.6 mm (1.4 in.) with roughness greater than 5 mm (0.2 in.) was observed to be enough for repair of NSC substrate when the horizontal interface shear stress demand was less than 1.38 MPa (0.2 ksi).

Comparison with Current Design Codes

The experimental results obtained from push-off tests were compared with calculated capacities using current AASHTO, ACI, and PCI design guidelines. Only AASHTO code has provision for calculating interface shear capacity for specimens without interface reinforcement. For AASHTO, ACI, and PCI provisions, the measured yield strength of the interface reinforcement was used for "f_y" instead of the grade of the interface reinforcement typically used in design equations. The design provisions were found to be conservative as shown in Fig. 13. The AASHTO guidelines, which takes cohesion into account, is more accurate in predicting shear capacity of the specimens compared with the other two provisions.

Though the code provisions are conservative in predicting the shear strength capacity, some of the experimental observations show their limitations in accurately representing interface shear behavior. The AASHTO, ACI, and PCI design equations assume that the interface reinforcement is at yield at peak shear capacity. The strain readings of interface reinforcement in N-U-WI-2 were below yield at the peak shear capacity. However, specimen N-U-WI-2 had interface shear strength 145% and 230% higher than the strength calculated using AASHTO and ACI design guidelines, respectively. This could be due to the grooved roughness texture at the interface, which facilitates transfer of shear force through mechanical action. In addition, for specimens with the same interface reinforcement ratio, the higher interface roughness could result in greater shear friction resistance at lower tensile strains in interface reinforcements. Harris et al. (2013) had also previously reported this lag in yielding of interface reinforcement with respect to peak shear capacity. Similarly, results from push-off tests conducted by Sneed et al. (2016) using LWC also indicate that the interface reinforcement might not yield at peak capacity when both interface roughness and reinforcement ratio are increased. However, AASHTO, ACI, and PCI guidelines assume yield of interface reinforcement at peak load for all cases. Further study with increased reinforcement ratio and interface roughness depth is required to examine this case.

The coefficient of friction "μ" used in design codes is an empirical fit across test results and not the actual friction property of the interface surfaces (Harris et al. 2013). The shear capacity in WI and PI specimens increased by 1.6 and 1.4 times, respectively, even when the reinforcement area was increased by two times. The present design guidelines suggest the increment of shear capacity to be linearly proportional to the increment in area of interface reinforcement. The coefficient of friction used in the design guidelines should be further investigated to accurately capture the effects of increasing reinforcement ratio.

Conclusions and Recommendations

A total of ten push-off tests and four composite beam flexural tests were carried out to investigate the interface behavior at NSC-UHPC interfaces. The following conclusions and recommendations are made based on the test observations:

- In general, the interface shear capacity increases with an increase in the roughness depth and interface reinforcement ratio. The increase in shear capacity was not linearly proportional to the increase in interface reinforcement ratio.
- The behavior of interface reinforcement was dependent on surface preparation and reinforcement ratio. As roughness depth and reinforcement ratio increases, tensile strains in the interface reinforcement, measured at the peak interface shear capacity decreased.
- Current AASHTO, ACI, and PCI design guidelines were found to be conservative in estimating the interface shear capacity of NSC-UHPC composites.
- The observations from push-off tests showed that specimens with higher roughness and interface reinforcement amount exhibited lower slip at the peak load, higher stiffness, higher residual strength and higher ductility. Thus, such interface configurations are recommended for repair purposes.
- Further study is required to calibrate cohesion and coefficient friction "μ" to accurately predict interface shear capacity across various roughness depths and interface reinforcement ratios.

Data Availability Statement

All data, models, and code generated or used during the study appear in the published article.

Acknowledgments

The study reported in this paper is supported by the National Science Foundation through the Engineering for Natural Hazards (ENH) program (Grant No. 1662963). Any opinions, findings, and conclusions expressed in this paper are those of the authors, and do not necessarily represent those of the sponsor. The authors would like to thank the reviewers for their insightful comments, which helped to improve the paper. The authors would also like to acknowledge help received from Collin Sewell during specimen fabrication and test setup in the Large Scale Structures Lab at University of Alabama. The authors are thankful to Dr. Ali A. Semendary for his valuable inputs in preparation of the manuscript. In addition, the authors are thankful to Brian Muni from the University of Central Florida for his help during some of the experimental activities as part of Research Experience for Undergraduates (REU) program.

References

Aaleti, S., and S. Sritharan. 2014. "Design of ultrahigh-performance concrete waffle deck for accelerated bridge construction." *Transp. Res. Rec.* 2406 (1): 12–22. https://doi.org/10.3141/2406-02.

Aaleti, S., and S. Sritharan. 2019. "Quantifying bonding characteristics between UHPC and normal-strength concrete for bridge deck application." *J. Bridge Eng.* 24 (6): 04019041. https://doi.org/10.1061/(ASCE)BE.1943-5592.0001404.

AASHTO. 2017. *AASHTO LRFD bridge design specifications*. 8th ed. Washington, DC: AASHTO.

ACI (American Concrete Institute). 2014. *Building code requirements for structural concrete and commentary*. ACI 318-14. Farmington Hills, MI: ACI.

ASCE. 2017. "Bridges, 2017 Infrastructure report card." Accessed October 10, 2019. https://www.infrastructurereportcard.org/wp-content/uploads/2017/01/Bridges-Final.pdf.

ASTM. 2013. *Standard test methods for tension testing of metallic materials*. ASTM E8. West Conshohocken, PA: ASTM.

ASTM. 2020. *Standard test method for compressive strength of cylindrical concrete specimens*. ASTM C39. West Conshohocken, PA: ASTM.

Banta, T. E. 2005. "Horizontal shear transfer between ultra high performance concrete and lightweight concrete." M.S. thesis, Dept. of Civil and Environmental Engineering, Virginia Polytechnic Institute and State Univ.

Berger, R. 1983. "Full-Depth modular precast, prestressed bridge decks." *Transp. Res. Rec.* 903: 52–59.

Birkeland, P. W., and H. W. Birkeland. 1966. "Connection in precast concrete connections." *J. Am. Concr. Inst.* 63 (3): 345–368.

Crane, C. K. 2010. "Shear and shear friction of ultra-high performance concrete bridge girders." Ph.D. thesis, School of Civil and Environmental Engineering, Georgia Institute of Technology.

FHWA (Federal Highway Administration). 2011. *Bridge preservation guide*. Mclean, VA: FHWA.

FHWA (Federal Highway Administration). 2013. *Ultra-high performance concrete: A state-of-the-art report for the bridge community*. Mclean, VA: FHWA.

Graybeal, B., and M. Davis. 2008. "Cylinder or cube: Strength testing of 80 to 200 MPa (11.6 to 29 ksi) ultra-high-performance fiber-reinforced concrete." *ACI Mater. J.* 105 (6): 603.

Harris, K. A., Z. Gabriel, and S. Bahram. 2013. "Toward an improved understanding of shear-friction behavior." *ACI Struct. J.* 109 (6): 835–897.

Hofbeck, J. A., I. O. Ibrahim, and A. H. Mattock. 1969. "Shear transfer in reinforced concrete." *ACI J. Proc.* 66 (2): 119–128.

Jang, H.-O., H.-S. Lee, K. Cho, and J. Kim. 2017. "Experimental study on shear performance of plain construction joints integrated with ultra-high performance concrete (UHPC)." *Constr. Build. Mater.* 152: 16–23. https://doi.org/10.1016/j.conbuildmat.2017.06.156.

Mast, R. F. 1968. "Auxiliary reinforcement in concrete connections." *J. Struct. Div.* 94 (6): 1485–1504.

Munoz, M. A., D. K. Harris, T. M. Ahlborn, and D. C. Froster. 2014. "Bond performance between ultrahigh-performance concrete and normal-strength concrete." *J. Mater. Civ. Eng.* 26 (8): 04014031. https://doi.org/10.1061/(ASCE)MT.1943-5533.0000890.

PCI (Precast/Prestressed Concrete Institute). 2010. *PCI design handbook*. Chicago, IL: PCI.

Ronanki, V. S., S. Aaleti, and J. P. Binard. 2019. "Long-span hybrid precast concrete bridge girder using ultra-high performance concrete and normal weight concrete." *PCI J.* 64 (6): 45–61. https://doi.org/10.15554/pcij64.6-02.

Santos, P. M., and E. N. Julio. 2014. "Interface shear transfer on composite concrete members." *Struct. J.* 111 (1): 113–122.

Sarkar, J. 2010. "Characterization of the bond strength between ultra high performance concrete bridge deck overlays and concrete substrates." M.S. thesis, Civil and Environmental Engineering, Michigan Technological Univ.

Sharma, S., S. Aaleti, and T. N. Dao. 2019. "An experimental and statistical study of normal strength concrete (NSC) to ultra high performance concrete (UHPC) interface shear behavior." In *Proc., 2nd Int. Interactive Symp. on UHPC*, 1–11. Ames, IA: Iowa State University Digital Press.

Silfwerbrand, J. 2017. "Bonded concrete overlays." *Concr. Int.* 39 (5): 31–36.

Sneed, L. H., S. Wermager, and K. Krc. 2016. *Interface shear transfer of lightweight aggregate concretes with different lightweight aggregates*. Chicago, IL: Precast/Prestressed Concrete Institute.